

## Mathematical modelling of atom loss in delivery tubing

R. SCOTT DANIELS AND DONALD C. WIGFIELD<sup>1</sup>

*The Ottawa-Carleton Chemistry Institute, Department of Chemistry, Carleton University,  
Ottawa, Ont., Canada K1S 5B6*

AND

KENNETH S. WILLIAMS

*Department of Mathematics and Statistics, Carleton University, Ottawa, Ont., Canada K1S 5B6*

Received July 10, 1991<sup>2</sup>

R. SCOTT DANIELS, DONALD C. WIGFIELD, and KENNETH S. WILLIAMS. *Can. J. Chem.* **70**, 1978 (1992).

A mathematical model is presented to establish a relationship between the quantity of trace analyte vapor lost to the surface of delivery tubing and the tubing diameter, while in transit between stages of an instrument. Cold-vapor atomic absorption spectrometry for mercury, hydride generation techniques, and interfaces like the interface between electrothermal vaporization and inductively coupled plasma mass spectrometry all risk significant analyte loss before measurement. The results of this modelling substantiate the results of limited experimental work published elsewhere suggesting the use of the smallest possible tubing diameter for the delivery of atomic vapor through a tube. This diameter is calculable using Poiseuille's formula. Using this model, kinetic theory, and experimental data, the sticking probability for mercury on latex tubing is calculated to be approximately  $1.6 \times 10^{-6}$ .

R. SCOTT DANIELS, DONALD C. WIGFIELD et KENNETH S. WILLIAMS. *Can. J. Chem.* **70**, 1978 (1992).

On présente un modèle mathématique permettant d'établir une relation entre le diamètre du tube et la quantité d'une trace à analyser en phase vapeur qui est perdue sur la surface du tube de transfert entre deux stades d'un instrument. Dans les techniques de génération d'hydruure de la spectroscopie d'absorption atomique de vapeurs froides pour le mercure et dans les interfaces comme celle qui existe entre la vaporisation électrothermique et la spectrométrie de masse aux plasmas couplés d'une façon inductive, il existe des risques importants de perte des produits à analyser. Les résultats de notre modèle permettent de circonstancier les résultats expérimentaux limités qui ont été publiés ailleurs et qui suggèrent qu'il est utile d'utiliser des tubes ayant des diamètres les plus faibles que possible pour transférer une vapeur atomique à travers un tube. On peut calculer ce diamètre à l'aide de la formule de Poiseuille. Utilisant ce modèle, la théorie cinétique et les données expérimentales, on a calculé que le probabilité d'adhérence du mercure sur un tube de latex est approximativement  $1,6 \times 10^{-6}$ .

[Traduit par la rédaction]

### I. Introduction

The substance of this communication lies in a single question; that is, for a given standard flow rate of a carrier gas containing a trace analyte, which is the best for minimizing analyte loss to the surface of the delivery tubing: a small diameter tube, a large diameter tube, or is there an optimum diameter?<sup>3</sup>

Cold-vapor atomic absorption spectrometry, hydride generation techniques, electrothermal vaporization inductively coupled plasma mass spectrometry, and gas chromatography graphite furnace atomic absorption share one thing in common: the transport of trace molecular or atomic vapor, or aerosols, through delivery tubing. To ensure optimum analytical sensitivity, it is necessary to provide conditions to minimize analyte loss due to surface interactions along the walls of the delivery tubing. An earlier communication addressed the question of tubing type and optimum tubing diameter from an experimental perspective (1). Due to a limited number of available tubing diameters for testing, it was felt that a mathematical model of atom loss in tubing, particularly as a function of tubing diameter and flow rate, would add further justification to, and understanding of, the trends observed for the limited number of diameters tested. In ad-

dition, this model would permit predictions beyond the scope of readily available tubing diameters. A brief summary of transport efficiency and particle size is given by Lubman (2). Although omitting a sticking probability factor that is introduced in this model, a solution to the ratio of the number of particles at the exit of a tube to the number at the entrance is given by Gormley and Kennedy (3). Their model is most applicable to mass transport of larger particles and aerosols transported by a carrier gas through a horizontal tube.

The presentation of this model will be in two parts: a simple intuitive approach will be given, followed by a more detailed model of atom loss.

### II. Experimental section

An evaluation of the atom loss dependence on the tubing diameter used 3.7 m lengths of latex tubing (Fisher Cat. No. 14-150) of varying diameters. While the tube was attached to the inlet of the spectrometer, and ambient air was being drawn by a pump through the tubing, 10  $\mu\text{L}$   $\text{Hg}^0$  vapor (21–23°C, approximately 0.15 ng) injections were made alternately at a port directly adjacent to the inlet to the spectrometer and at an injection port attached to the end of the 3.7 m length of tubing.

#### Apparatus

A Laboratory Data Control/Milton Roy UVD 253.7 nm spectrometer was used for measuring the integrated absorbance signals. The fluid flow cell from the UVD monitor was removed and the detector was fixed to the end of a 30-cm double beam gas flow cell. Data acquisition was performed using a Jones Chromatography 6000 data system. Mercury vapor injections were performed using a 10- $\mu\text{L}$  gas-tight syringe (Hamilton, 1801RN-3). The mercury vapor was housed in a septum-sealed 25-mL volumetric flask

<sup>1</sup>Author to whom correspondence may be addressed.

<sup>2</sup>Revision received March 2, 1992.

<sup>3</sup>There is an analogous question, and an apparent lack of a scientific answer for this question, pertaining to minimizing the heat loss during the transport of a warm gas through optimum piping diameters.

containing 5 mL of elemental mercury. Temperature-sensitive fluctuations of the vapor pressure of mercury were minimized by partially immersing the volumetric flask in water contained in a double-insulated 200-mL beaker. The flow rate was monitored using a bubble-meter calibrated mass flow meter (Matheson 0–2000 standard mL min<sup>-1</sup>, model 81111-0423).

### III. Results and discussion

#### III.1. A simplified perspective of atom loss

Consider a segment of tubing of length  $l$  (cm), diameter  $d$  (cm), standard flow rate  $f$  (mL min<sup>-1</sup>), volume  $v$  (cm<sup>3</sup>), and internal surface area,  $s$  (cm<sup>2</sup>). As a plug of vapor traverses the length of the tube there is some function  $h$ , describing atom loss, that depends both on the mean atom residence time  $\tau$  (s) (4), and the tube surface to volume ratio  $s/v$ , eq. [1].

$$[1] \quad \text{loss} = h\left(\tau, \frac{s}{v}\right) \\ = h\left(\frac{\pi l d^2}{4f}, \frac{4}{d}\right)$$

$$[2] \quad \text{loss} = h_1(d)$$

Since the standard flow rate is to be considered constant, then the new loss function  $h_1$ , eq. [2], is some unknown function of the delivery tube diameter. In eq. [1] it is not immediately clear how  $\tau$  and  $s/v$  will be a function of atom loss, but it is reasonable to argue that an increased atom residence time, and (or) an increased surface to volume ratio (i.e., decreased diameter), would result in increased atom loss. A longer atom residence time would give a higher probability of a surface adsorption, and the greater the amount of surface, the higher would be the probability of a surface interaction. Clearly then, as the tube diameter is varied, these two factors act in opposition insofar as atom loss is concerned. To illustrate this Fig. 1 shows how  $\tau$  and  $s/v$  vary with the tube diameter at a constant flow rate. If the loss function is an algebraic sum of the contributions from  $\tau$  and  $s/v$  (curve 3, a simplistic view, yet mathematically incorrect), then there would be a local minimum in the loss function versus tube radius. This will be shown to be incorrect.

To overcome the inadequacies of this simplified view of atom loss, a detailed model of atom loss will permit a rigorous evaluation of  $h_1$ .

#### III.2. A detailed model of atom loss

The development of this detailed atom loss model entails 12 assumptions listed below:

1.  $N_0$  mercury atoms are instantaneously injected into a flow of ambient nitrogen carrier gas such that the mercury atoms are evenly distributed across a plug volume of radius  $r$  and length  $x$ .

2. In the time increment  $1/Z$ , all atoms a distance  $\lambda$  or less from the tube surface are lost to the tube wall.  $Z$  is the collision frequency and  $\lambda$  is the mean free path of mercury atoms with nitrogen molecules under ambient conditions. This assumption disregards the sticking probability  $\rho$ , and the kinetic geometry term,  $g$ . See Appendix.

3. No pressure drop occurs along the tube length, for all tube radii and flow rates, omitting the Poiseuille pressure drop.

4. Following each  $1/Z$  increment, the remaining atoms

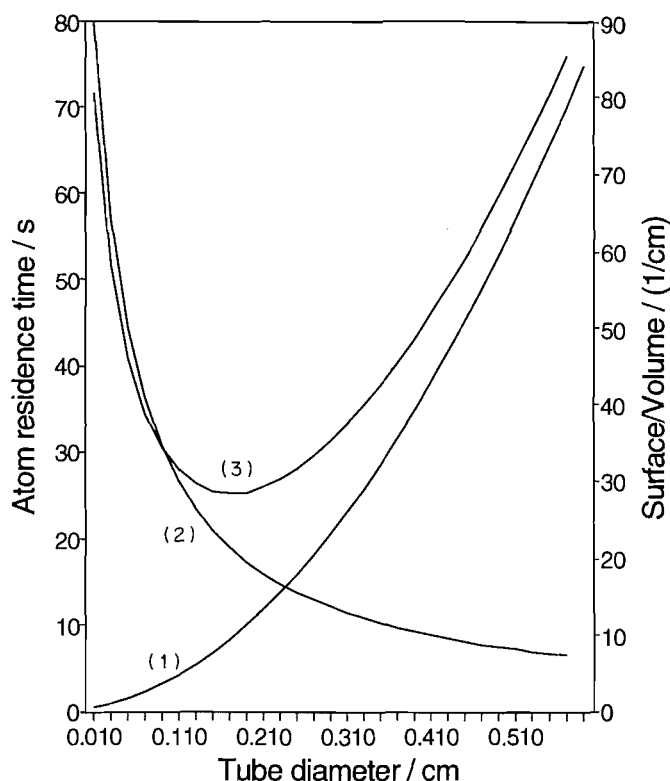


Fig. 1. Variation of atom residence time (1); surface to volume ratio (2); and their sum<sup>4</sup> (3); with tube diameter at 100 mL min<sup>-1</sup>.

instantaneously redistribute themselves across the plug volume  $v$ .

5. No axial diffusional broadening of the plug occurs as it moves along the length of the tube.

6. There will exist a uniform non-parabolic velocity distribution along the tube cross section.

7. The tube wall surface is ideal: no eddies.

8. Syringe injection produces a homogeneous disk distribution of mercury vapor in nitrogen.

9. Nitrogen,  $N_2(g)$ , and mercury,  $Hg^0(g)$ , behave as ideal gases.

10. Flow is generated by draw from the atmosphere, through the tubing, to a vacuum pump.

11. The tube radius will not be less than the mean free path  $\lambda$ .

12. The tube wall is flat, not curved. See Appendix.

The philosophy adopted for developing this model has been to obtain a mathematical solution for the simplest case: making all the assumptions above, for model 1, then removing the assumptions sequentially until it is felt that there is sufficient agreement with experimental data. This outlook has resulted in three models presented in the order of making (1) all the assumptions above, (2) assumptions 3–8 above, and (3) assumptions 4–8 above.

#### III.3. Model 1

The goal of model 1 is to obtain a mathematical expression for the ratio of the number of atoms lost at the tube sur-

<sup>4</sup>Arithmetically incorrect, but presented for illustrative purposes.

TABLE 1. Model 1: incremental atom loss

Time	Number of atoms lost, $N$	Number of atoms remaining
0	0	$N_0$
$1/Z$	Atom density $\times$ rim volume $\frac{N_0}{v} [x\pi\{r^2 - (r - \lambda)^2\}] = N_0K$ where $K = \left[ \frac{x\pi\{r^2 - (r - \lambda)^2\}}{v} \right]$ $= \frac{\text{rim volume}}{\text{plug volume}}$	$N_0(1 - K)$
$2/Z$	$N_0K(1 - K)$	$N_0(1 - K)^2$
$3/Z$	$N_0K(1 - K)^2$	$N_0(1 - K)^3$
$4/Z$	$N_0K(1 - K)^3$	$N_0(1 - K)^4$

face to the number of atoms before any loss,  $N/N_0$ . The following notation will be used:

Term	Symbol	Units
Carrier gas	$N_2$	
Carrier gas viscosity	$\mu$	$\text{kg m}^{-1} \text{s}^{-1}$
Flow rate	$f$	$\text{m}^3 \text{s}^{-1}$
Tube length	$l$	m
Tube radius	$r$	m
Plug length	$x$	m
Plug volume	$v$	$\text{m}^3$
Plug, atom residence time	$\tau$	s
Mean free path of $\text{Hg}^0(\text{g})$ in $\text{N}_2(\text{g})$	$\lambda$	m
Collision frequency, $\text{Hg}^0(\text{g})$ with $\text{N}_2(\text{g})$	$Z$	$\text{s}^{-1}$

The total number of atoms lost is the sum of the number of atoms lost in each of  $\eta$  time increments of  $1/Z$ , where  $\eta$  is the floor<sup>5</sup> of the product of the collision frequency  $Z$  and the plug residence time  $\tau$ . Table 1 lists the number of atoms lost to the tube wall, and the number of atoms remaining, for each of the first four of  $\eta$ ,  $1/Z$  increments of time. The number of atoms lost in the first time increment of  $1/Z$  is the number of atoms contained in the rim of the disk whose thickness is  $\lambda$ , the mean free path of a mercury atom in nitrogen (approximately 45.7 nm, for 20°C), and whose length is  $x$ . This number is the product of the rim volume,  $x\pi\{r^2 - (r - \lambda)^2\}$  and the initial atom density  $N_0/v$ .

Similarly, the number of atoms lost at the time  $2/Z$  is the product of the new atom density  $(N_0 - N_0K)/v$  and the rim volume. As shown in Table 1, this number is merely the product of the remaining number of atoms in the plug volume  $(N_0 - N_0K)$  and  $K$ , where  $K$  is the ratio of the rim volume to the plug volume.

The total number  $N$  of atoms lost is

$$[3] \quad N_0K \sum_{n=0}^{n=\eta} (1 - K)^n$$

where

<sup>5</sup>The floor operator ( $\{x\}$ ) takes the integer portion of its argument; for example,  $\{3.7\} = 3$ .

$$[4] \quad \eta = \lfloor Z \times \tau \rfloor = \left\lfloor \frac{Z\pi lr^2}{f} \right\rfloor$$

Summing the geometric series gives eq. [5],

$$[5] \quad \frac{N}{N_0} = 1 - [1 - K]^{\eta+1} \\ = 1 - \left\{ 1 - \frac{x\pi[r^2 - (r - \lambda)^2]}{v} \right\}^{\eta+1} \\ = 1 - \left[ 1 - \frac{(2r\lambda - \lambda^2)}{r^2} \right]^{\lfloor Z\pi lr^2/f \rfloor + 1}$$

where  $v = x\pi r^2$ .

Figure 2 is a plot of the adsorptional loss,  $N/N_0$ , versus the log of the tube radius. This model, like the simplified view of Fig. 1, also predicts a local minimum in the loss function versus tube radius. In model 1, increased tube length has two effects: a shift in optimum diameter to larger radii, and greater losses at all radii.

#### III.4. Model 2

Model 2 corrects for the certainty that not every atom striking the tube surface is lost. It also corrects for the fact that not all atoms at a distance  $\lambda$  or less from the tube wall will have trajectories in the direction of the wall. The correction terms will be  $\rho$  and  $g$  respectively. In fact, only one quarter of the atoms within the distance  $\lambda$  from the wall will strike the wall ( $g = \frac{1}{4}$ , Appendix). Table 2 is a modification of Table 1, taking into account the sticking probability  $\rho$ , and the geometry factor,  $g$ .

Summing the geometric series as in model 1, and substitution of  $\frac{1}{4}$  for  $g$ , gives eq. [6],

$$[6] \quad \frac{N}{N_0} = 1 - \left[ 1 - \frac{\rho(2r\lambda - \lambda^2)}{4r^2} \right]^{\lfloor Z\pi lr^2/f \rfloor + 1}$$

Figure 3 is a plot of the adsorptional loss,  $N/N_0$ , versus the log of the tube radius, for  $\rho$  values of  $10^{-4}$ ,  $10^{-2}$ , and 1. Like the previous model, this model also predicts the existence of a local minimum in the loss functions of Fig. 3 at radii of  $7.6\lambda$ .

According to this intermediate and still very naive model,

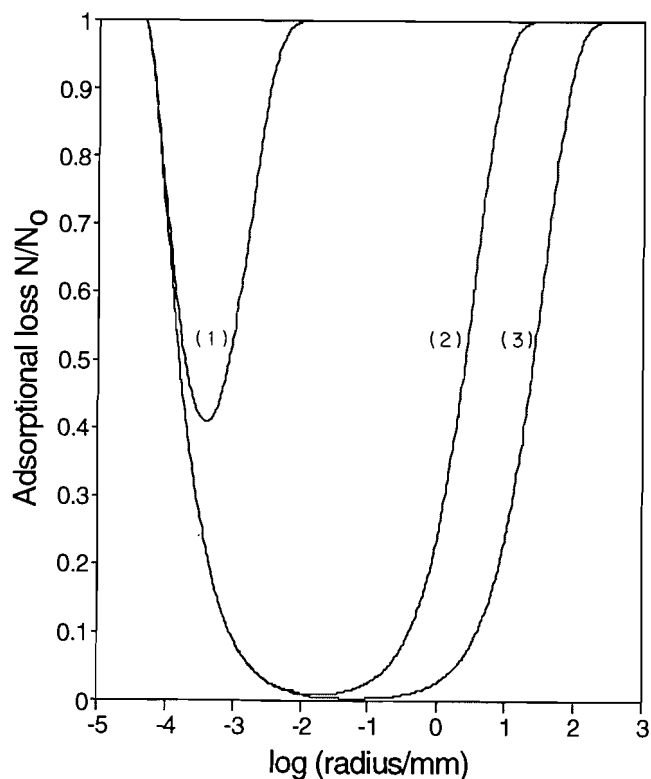


FIG. 2. Atom loss model 1. Plot of  $N/N_0$  versus  $\log(\text{tube radius})$  for  $100 \text{ mL min}^{-1}$  and tube lengths/nm: (1)  $10^{-6}$ ; (2) 40; (3) 400.

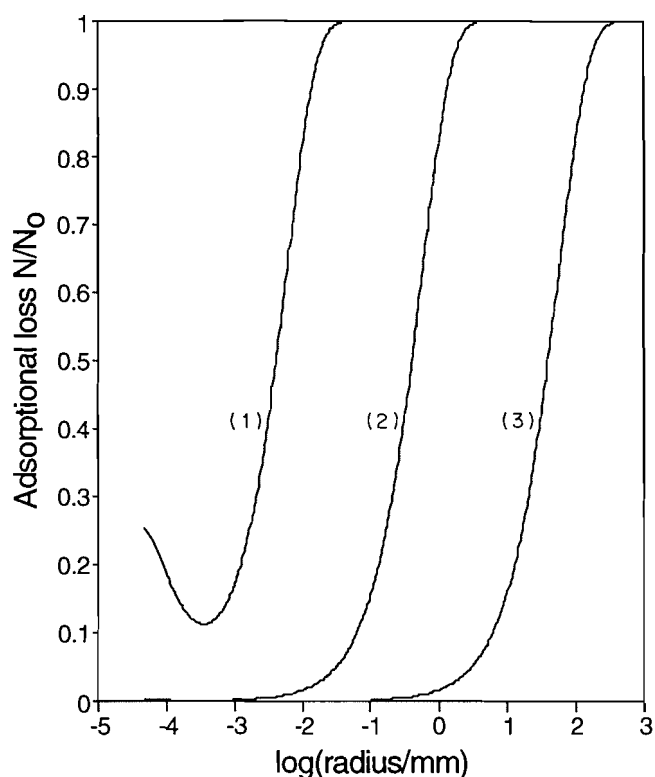


FIG. 3. Atom loss model 2. Plot of  $N/N_0$  versus  $\log(\text{tube radius})$  for:  $f = 100 \text{ mL min}^{-1}$ ,  $l = 1.0 \text{ mm}$ , and sticking probability,  $\rho$ : (1) 1; (2)  $10^{-2}$ ; (3)  $10^{-4}$ .

TABLE 2. Model 2: incremental atom loss

Time	Number of atoms lost, $N$
$1/Z$	$g\rho \times \text{atom density} \times \text{rim volume}$ $g\rho \frac{N_0}{v} \{x\pi[r^2 - (r - \lambda)^2]\} = \rho N_0 K$ where $K = \left\{ \frac{x\pi[r^2 - (r - \lambda)^2]}{v} \right\}$
$2/Z$	$g\rho N_0 K(1 - g\rho K)$
$3/Z$	$g\rho N_0 K(1 - g\rho K)^2$
$4/Z$	$g\rho N_0 K(1 - g\rho K)^3$

the limiting tube radius would be  $\lambda$ , when, in this limit, the loss,  $N/N_0$ , would approach a value of  $\rho g$ . Very small diameters lead to the ludicrous situation of linear atomic trajectories surpassing the speed of light: in fact,  $3c$ , for a flow rate of  $100 \text{ mL min}^{-1}$  and a tube radius of  $\lambda/2$ ! The real limiting diameter would be the diameter, calculable from the Poiseuille equation, for a given standard flow rate through a defined length of tubing, and the condition of a pressure drop of 1 atmosphere along the length of the tube. This limiting diameter is best illustrated in Model 3.

### III.5. Model 3

This, the third and final model, takes into account the pressure drop at some distance  $y$  along the tube length  $l$ . As the pressure drops in the direction of the vacuum pump, from ambient pressure  $P_1$  at the open end of the tube to some lower pressure  $P_2$  at the pump end of the tube, the kinetic properties  $Z$ , the flow rate  $f$ , and  $\lambda$  change.  $P_2$  is a function of  $y$ .

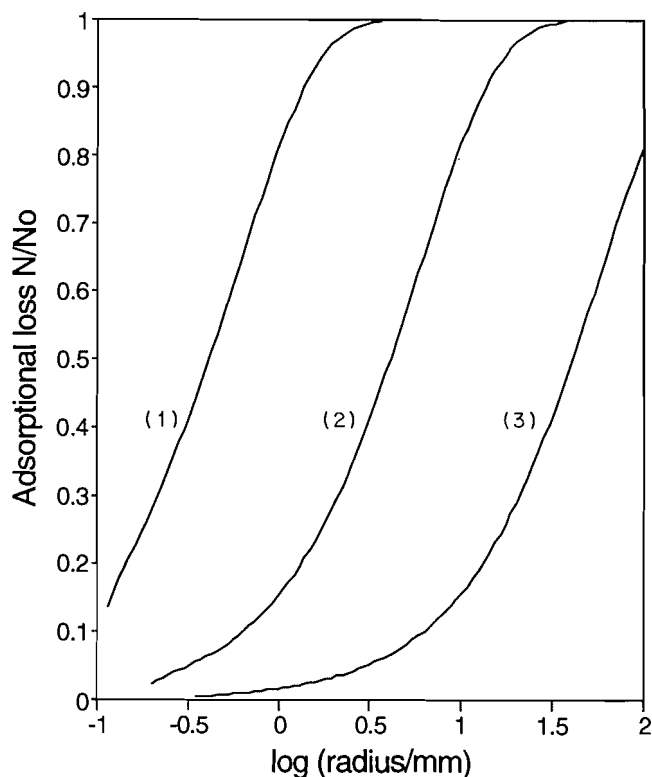


FIG. 4. Atom loss model 3. Plot of  $N/N_0$  versus  $\log(\text{tube radius})$  for:  $l = 1.0 \text{ m}$ ,  $\rho = 10^{-6}$ , and  $f/(\text{mL min}^{-1})$ : (1) 10; (2) 100; (3) 1000.

To correct for this, the mean values of  $Z$ ,  $f$ , and  $\lambda$  are calculated and used in place of the fixed values in model 2. The variables  $Z'$ ,  $f'$ , and  $\lambda'$ , are the values of  $Z$ ,  $f$ , and  $\lambda$  respectively under ambient conditions, and are defined collectively in eq. [7] as follows:

$$[7] \quad \bar{Z} = \frac{1}{l} \int_{y=0}^{y=l} Z' \frac{P_2}{P_1} dy, \quad Z = Z' \times \left( \frac{P_2}{P_1} \right)$$

$$\bar{f} = \frac{1}{l} \int_{y=0}^{y=l} f' \frac{P_1}{P_2} dy, \quad f = f' \times \left( \frac{P_1}{P_2} \right)$$

$$\bar{\lambda} = \frac{1}{l} \int_{y=0}^{y=l} \lambda' \frac{P_1}{P_2} dy, \quad \lambda = \lambda' \times \left( \frac{P_1}{P_2} \right)$$

and  $dy$  is some infinitesimal of the tube length  $l$ . Solving the Poiseuille equation:

$$[8] \quad f' = \frac{(P_1^2 - P_2^2)\pi r^4}{16\gamma\mu P_1}$$

for  $P_2$ , and substitution into the previous integral eqs. [7] gives equation set [9].

$$[9] \quad \bar{Z} = \frac{Z'}{P_1 l} \int_{y=0}^{y=l} \sqrt{P_1^2 - \frac{16\mu P_1 f' y}{\pi r^4}} dy$$

$$\bar{f} = \frac{f' P_1}{l} \int_{y=0}^{y=l} \frac{1}{\sqrt{P_1^2 - \frac{16\mu P_1 f' y}{\pi r^4}}} dy$$

$$\bar{\lambda} = \frac{\lambda' P_1}{l} \int_{y=0}^{y=l} \frac{1}{\sqrt{P_1^2 - \frac{16\mu P_1 f' y}{\pi r^4}}} dy$$

The solution for these integral equations is given in eq. [10].

$$[10] \quad \bar{Z} = \frac{Z' \pi r^4}{24 P_1^2 l \mu f'} \left[ P_1^3 - \left( P_1^2 - \frac{16\mu P_1 f' l}{\pi r^4} \right)^{3/2} \right]$$

$$\bar{f} = \frac{\pi r^4}{8 l \mu} \left[ P_1 - \sqrt{P_1^2 - \frac{16\mu P_1 f' l}{\pi r^4}} \right]$$

$$\bar{\lambda} = \frac{\lambda' \pi r^4}{8 \mu l f'} \left[ P_1 - \sqrt{P_1^2 - \frac{16\mu P_1 f' l}{\pi r^4}} \right]$$

Substitution of these average values of  $Z$ ,  $f$ , and  $\lambda$  into the general solution from model 2 gives eq. [11], the general solution for model 3.

$$[11] \quad \frac{N}{N_0} = 1 - \left\{ 1 - \frac{\rho a r^4 \left[ P_1 - \sqrt{P_1^2 - \frac{b}{r^4}} \right] \left[ 2r - a r^4 \left( P_1 - \sqrt{P_1^2 - \frac{b}{r^4}} \right) \right]}{4r^2} \right\}^{[c r^2 (2P_1^2 + P_1 \sqrt{P_1^2 - (b/r^4)} - (b/r^4))] + 1}$$

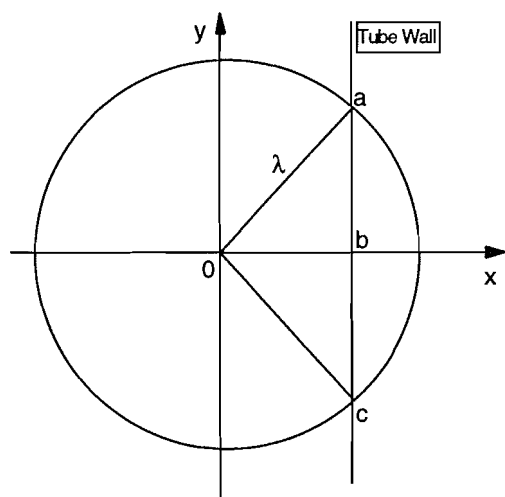
where

$$[12] \quad a = \frac{\lambda' \pi}{8 \mu l f'}, \quad b = \frac{16 \mu P_1 f' l}{\pi}, \quad c = \frac{Z' \pi l}{3 P_1^2 f'}$$

A plot of this equation using  $l = 1.0$  m,  $\rho = 10^{-6}$ , and  $\mu = 1.76 \times 10^{-5}$  kg m<sup>-1</sup> s<sup>-1</sup> is given in Fig. 4 for  $f' = 10, 100$ , and 1000 mL min<sup>-1</sup>. The model 3 functions are truncated at radii predicted by the Poiseuille equation. These limiting radii get

TABLE 3. Estimation of the latex sticking probability,  $\rho$ , by comparison of experimental and theoretical loss data

Flow rate (mL min <sup>-1</sup> )	Internal radius (mm)	Loss $N/N_0$			
		Experimental		Theory: model 3	
		Day 1	Day 2	$\rho = 1.6 \times 10^{-6}$	$\rho = 1.6 \times 10^{-7}$
50	0.8	0.77±0.01	0.82±0.02	0.80	0.18
	1.6	0.84±0.01	0.87±0.01	0.96	0.33
	3.95	0.93±0.01	0.96±0.01	1.00	0.63
100	0.8	0.65±0.01	0.67±0.02	0.55	
	1.6	0.73±0.01	0.78±0.01	0.80	
	3.95	0.79±0.01	0.86±0.01	0.98	
200	0.8	0.48±0.01	0.51±0.02	0.33	
	1.6	0.52±0.03	0.62±0.01	0.53	
	3.95	0.59±0.01	0.63±0.02	0.86	
500	0.8	0.39±0.01	0.40±0.03	0.14	
	1.6	0.36±0.01	0.47±0.01	0.27	
	3.95	0.33±0.01	0.48±0.02	0.54	
1000	0.8	0.07±0.06	0.28±0.02	0.07	
	1.6	0.16±0.04	0.28±0.03	0.15	
	3.95	0.20±0.03	0.29±0.06	0.32	
1500	0.8	0.03±0.05	0.16±0.07	0.05	
	1.6	0.15±0.04	0.18±0.01	0.10	
	3.95	0.27±0.01	0.19±0.02	0.23	

FIG. 5. Solution for the geometry term  $g$ : the fraction of atoms within the distance  $\lambda$  from the tube wall that strike the wall.

smaller as the flow rate decreases. Just as predicted by the experimental data of Table 3, the ideal conditions to minimize analyte loss to tubing surfaces are (1) use the smallest tube diameter possible, and (2) use the highest flow rate possible.

### III.6. Estimating a value of $\rho$ , the sticking probability for latex

Using the general solution of model 3 above, combined with experimental data for  $N/N_0$ , an estimate of the real value of  $\rho$  may finally be made. Variables are used in the model 3

solution of Table 3 according to the conditions that prevailed while data was collected. An estimate of  $\rho = 1.6 \times 10^{-6}$  gives model 3 solutions for  $N/N_0$  that agree satisfactorily with experimental values shown in Table 3. The mathematical model is more sensitive to a change in loss, with changing tube radii, than is observed experimentally. At higher flow rates, there is a larger uncertainty and poor reproducibility between days, in experimental values of  $N/N_0$ . This model, in addition to predicting trends, was expected to give values of  $\rho$ , at best, to within an order of magnitude of its real value. Calculated values are listed in Table 3 showing the model 3 estimates for  $N/N_0$  at 50 mL min<sup>-1</sup> and for three radii, when a value of  $\rho = 1.6 \times 10^{-7}$  was used, which varies by an order of magnitude from the best estimate of  $\rho$ .

### IV. Conclusions

The atom loss model has been developed to the point at which it predicts loss trends as a function of varied tube radii for all possible flow rates, sticking probabilities, and tube lengths. The primary trend, that is, trace analyte loss increases with increasing tube diameter, was confirmed with this model, and corroborates inferences by the solution proposed by Gormley and Kennedy (2). Further to this and in conjunction with experimental data, the model allowed the estimation of a sticking probability. For latex tubing it was found that only one mercury atom in 0.83 million ( $\rho = 1.2 \times 10^{-6}$ ) that strikes the tube wall surface actually remains adsorbed for a sufficient length of time to be termed "lost."

### V. Acknowledgements

We are grateful to Dr. Steve Brooks of the Department of Biology, Carleton University, and Mr. Andrew Forrest, P.Eng., for extensive discussions and contributions to this work.

1. R. S. Daniels and D. C. Wigfield. *Anal. Chim. Acta*, **248**, 575 (1991).
2. D. M. Lubman, *Lasers and mass spectrometry*. Oxford University Press, New York, 1990.
3. P. G. Gormley and M. Kennedy. *Proc. R. Irish Acad.* **52A**, 163 (1949).
4. J. Dedina. *Prog. Anal. Spectrosc.* **11**, 251 (1988).

### Appendix

#### Solution for the geometry term $g$ : the fraction of atoms within the distance $\lambda$ from the tube wall that strike the wall

In Fig. 5, consider a wall at some distance  $b$ ,  $0 \leq b \leq \lambda$ , from an atom at the origin.<sup>6</sup> On this microscale, where  $\lambda$  is the mean free distance travelled by a mercury atom before collision with a nitrogen molecule, the tube wall will be considered to be flat and not curved.

The geometry term,  $g$ , represents the probability that an atom, at some distance less than or equal to  $\lambda$  from a wall, will strike the wall before hitting a nitrogen molecule.  $g$  is the ratio of the average sector-area of a sphere swept out by revolving the curve  $y = (\lambda^2 - x^2)^{1/2}$ ,  $b \leq x \leq \lambda$ , for  $0 \leq b \leq \lambda$ , about the  $x$ -axis to the total sphere surface area  $4\pi\lambda^2$ .

The general area of a surface, a sector-area of a sphere, swept out by revolving the curve  $y = f(x)$ ,  $a \leq x \leq b$ , about the  $x$ -axis (5) is given in eq. [13].

$$[13] \quad \int_a^b 2\pi y \sqrt{1 + (y')^2} dx$$

Therefore eq. [14] gives the sector-area of a sphere swept out by revolving the curve  $y = (\lambda^2 - x^2)^{1/2}$ ,  $b \leq x \leq \lambda$ , about the  $x$ -axis, where  $\lambda$  is the sphere radius, and eq. [15] gives the general sector-area  $A_s$  swept out by revolving the curve  $y = (\lambda^2 - x^2)^{1/2}$  about the  $x$ -axis.

<sup>6</sup>It is more convenient to consider an atom at the origin and the wall at different distances from the origin, than the reverse case.

$$[14] \quad \int_b^\lambda 2\pi \sqrt{\lambda^2 - x^2} \sqrt{1 + \frac{x^2}{\lambda^2 - x^2}} dx$$

$$= \int_b^\lambda 2\pi \sqrt{\lambda^2 - x^2} \sqrt{\frac{\lambda^2}{\lambda^2 - x^2}} dx$$

$$= \int_b^\lambda 2\pi\lambda dx$$

$$= 2\pi\lambda(\lambda - b)$$

$$[15] \quad A_s = 2\pi\lambda(\lambda - x), \quad 0 \leq x \leq \lambda$$

Equation [16] gives the average  $\bar{A}_s$  of the general sector-area  $A_s$  swept out by revolving the curve  $y = (\lambda^2 - x^2)^{1/2}$  about the  $x$ -axis, for  $0 \leq x \leq \lambda$ .

$$[16] \quad \bar{A}_s = \frac{1}{\lambda} \int_0^\lambda A_s dx$$

$$= \frac{1}{\lambda} \int_0^\lambda 2\pi\lambda(\lambda - x) dx$$

$$= 2\pi \left[ \int_0^\lambda \lambda dx - \int_0^\lambda x dx \right]$$

$$= 2\pi \left[ \lambda^2 - \frac{\lambda^2}{2} \right]$$

$$= \pi\lambda^2$$

Therefore,  $g$ , eq. [17], is the ratio of  $\bar{A}_s$  to the total sphere surface area  $4\pi\lambda^2$

$$[17] \quad g = \frac{\bar{A}_s}{4\pi\lambda^2} = \frac{1}{4}$$